



# Finely dispersed palladium on silk-fibroin as an efficient and ligand-free catalyst for Heck cross-coupling reaction

Hakimeh Mirzaei | Hossein Eshghi | Seyed Mohammad Seyedi

Department of Chemistry, Faculty of Science, Ferdowsi University of Mashhad, Mashhad, Iran

## Correspondence

Hossein Eshghi, Department of Chemistry, Faculty of Science, Ferdowsi University of Mashhad, Mashhad, Iran.  
Email: heshghi@um.ac.ir

A palladium–fibroin complex (Pd/Fib.) was prepared by the addition of sonicated fibroin fiber in water to palladium acetate solution. Pd (OAc)<sub>2</sub> was absorbed by fibroin and reduced with NaBH<sub>4</sub> at room temperature to the Pd(0) nanoparticles. Powder-X-ray diffraction, scanning electron microscopy–energy-dispersive X-ray spectroscopy, Fourier transform-infrared, CHN elemental analysis and inductively coupled plasma-atomic emission spectroscopy were carried out to characterize the Pd/Fib. catalyst. Catalytic activity of this finely dispersed palladium was examined in the Heck coupling reaction. The catalytic coupling of aryl halides (-Cl, -Br, -I) and olefins led to the formation of the corresponding coupled products in moderate to high yields under air atmosphere. A variety of substrates, including electron-rich and electron-poor aryl halides, were converted smoothly to the targeted products in simple procedure. Heterogeneous supported Pd catalyst can be recycled and reused several times.

## KEYWORDS

cross-coupling, Heck reaction, ligand-free, palladium–fibroin catalyst

## 1 | INTRODUCTION

The arylation or vinylation of alkenes with aryl or vinyl halides, known as the Heck reaction, was discovered independently by Heck in the 1970s.<sup>[1]</sup> The palladium-catalyzed cross-coupling reaction is a versatile tool for the generation of carbon–carbon bonds.<sup>[2]</sup> There are many chemical and pharmaceutical intermediates with alkene structural units being synthesized by including use of the Heck reaction in the presence of Pd catalyst.<sup>[3]</sup> Therefore, tremendous attention has been given to develop a new and advantageous catalytic system for Pd-catalyzed reactions.<sup>[4]</sup> Several catalytic systems, including the homogenized and the heterogeneous palladium-based catalyst, have been designed and made. The problem with homogeneous catalysis is the difficulty in separating the catalyst from the reaction mixture and the impossibility of reusing it in consecutive reactions,

whereas heterogeneous catalysts have many advantages, such as stability of the catalyst, easy separation from the reaction mixture over completion of the reaction, a good recyclability, cost reduction and high catalytic activity.<sup>[5]</sup> Because the catalytic process takes place on a metal surface, nanoparticles (NPs) are much more reactive than the particulate metal counterpart due to their small sizes and large surface areas. But the overall performance of nanomaterials depends on the size, shape, textural parameters of the particles and supporting materials that these NPs are stabilized on.<sup>[6]</sup> Therefore, different types of materials, such as fibers, mesoporous materials, metal oxide, activated carbon, polymers and dendrimers, have been employed to support NPs.<sup>[7]</sup> Most of these supporting materials require surface activator ligands due to their low activity in the adsorption of metal NPs. All of these catalyst systems suffer from drawbacks of one kind or another, such as the high ligand sensitivity

toward air and moisture, the tedious multistep synthesis, hence the high cost of the ligands, the use of various additives, and the need for an inert atmosphere during the synthesis of the catalyst as well as during the reaction.<sup>[8]</sup> On the other hand, ligand-free catalytic systems have many advantages in term of operational and economic efficiency. Many researchers have focused studies on applying natural biopolymers, such as silk,<sup>[9]</sup> starch, cellulose and chitosan, as activated supports for metal particles.<sup>[10]</sup> Many of the electron-rich functional groups in the protein bind with the metal surface easily, leading to the bioconjugation. The main characteristic of these biopolymers is their high amine group content, leading to interesting chelating properties for metal cations.<sup>[11]</sup> Natural silk is composed of two primary proteins: silk fibroin (SF; approximately 75%) and sericine (approximately 25%).<sup>[12]</sup> In raw silk, sericine is positioned across the surface of two parallel fibroin fibers, which binds them together.<sup>[13]</sup> SF is a fibrous protein with a semi-crystalline structure that provides stiffness and strength. Sericine is a glue-like amorphous protein that acts as an adhesive binder to keep the structural integrity of the fibers. Sericine is soluble and can be removed by a thermochemical process known as degumming.<sup>[14]</sup> The formation of SF heavy metals (Cu, Cr, Zn, etc.) complexes has been studied to improve the mechanical properties of silk fibers, removing heavy metals from water and to purify the organically polluted water.<sup>[15]</sup> In terms of the catalyst, fibroin metal catalysts have been used for chemoselective hydrogenation, reduction reaction of p-nitrophenol, hydroxylation of phenols and oxygen reduction reactions.<sup>[16]</sup>

Herein, we report an easy methodology for the synthesis of a green and heterogeneous efficient palladium

catalyst system (palladium–fibroin; Pd/Fib.), in which fibroin is used as a stabilizer to hamper the high amount of Pd employed for the effective ligand-free palladium-catalyzed Heck reaction.

## 2 | EXPERIMENTAL

### 2.1 | General

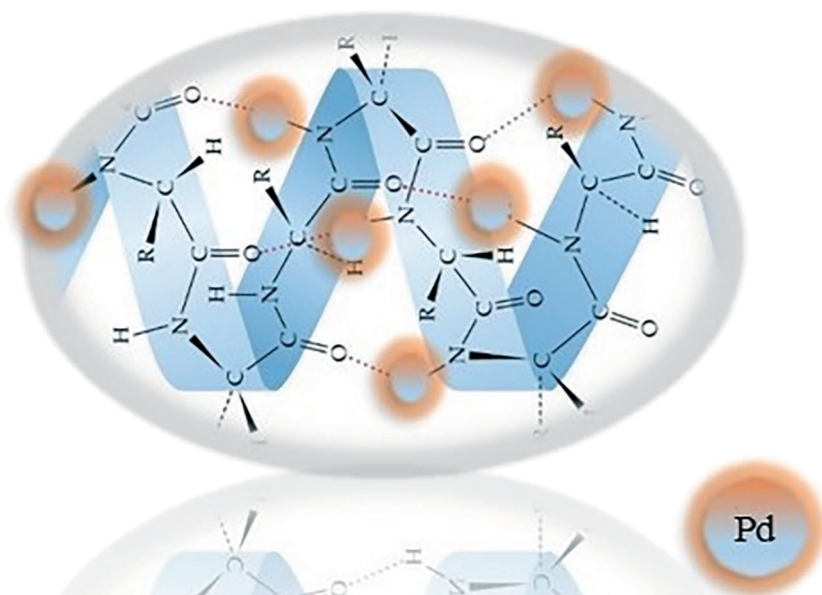
All chemicals were purchased from Merck, Fluka or Aldrich Chemical. The catalyst was synthesized and characterized according to the literature. All yields refer to isolated products. The products were characterized by comparing their physical data with those of known samples or by their spectral data.

### 2.2 | Preparation of support

The raw silk fibers were processed three times (30 min each time) in 0.5 wt.% Na<sub>2</sub>CO<sub>3</sub> solution at 80–90°C to remove sericine (degumming), rinsed with deionized water and dried at room temperature.

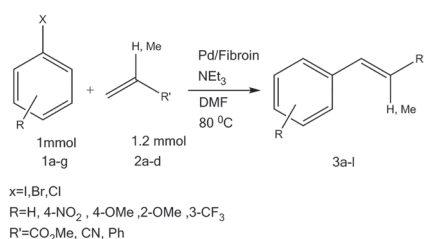
### 2.3 | Preparation of supported Pd<sup>0</sup> nanoparticles

The degummed fibroin (0.2 g) was dissolved in deionized water (10 cc) and sonicated for 10 min. Then, a solution of (0.1 M) palladium (II) acetate (5 cc) was added to the mixture and was stirred for 6 hr, leading to the absorption of Pd (II) on the fibroin surface. Afterwards, Pd (II)-



**SCHEME 1** Schematic representation of Pd/Fib. catalyst

supported fibroin was removed from the solution, and finally 0.1 M sodium borohydride solution (10 cc) was added dropwise to this and was stirred for 24 hr to provide a Pd (0)/Fib. catalyst. After completion of the reduction procedure, the catalyst was washed four times with water and ethanol (50:50) mixture and dried at room temperature. The Pd/Fib. catalyst structure is schematically shown in Scheme 1.



**SCHEME 2** General procedure for the synthesis of Heck adducts

## 2.4 | General procedure for the Heck coupling reaction

Aryl halide **1a-g** (1 mmol), alkene **2a-d** (1.2 mmol), triethylamine (1.2 mmol) and Pd/Fib. catalyst (0.05 mol%) were added to DMF (5 cc) and the reaction mixture was stirred at 80°C for the appropriate time. After completion of the reaction (monitored by thin-layer chromatography), the reaction mixture was cooled, diluted with chloroform (20 mL) and filtered to remove the catalyst. The organic layer was washed with water (40 mL  $\times$  2), dried over  $\text{MgSO}_4$  and concentrated under reduced pressure to obtain crude residue. The residue was purified by plate chromatography (hexane:ethylacetate) to afford the corresponding Heck adduct **3a-l** in moderate to high yields (Scheme 2).

All of the Heck coupling products are known, so these products were identified by comparison of their physical data with those of authentic samples. In spite of physical

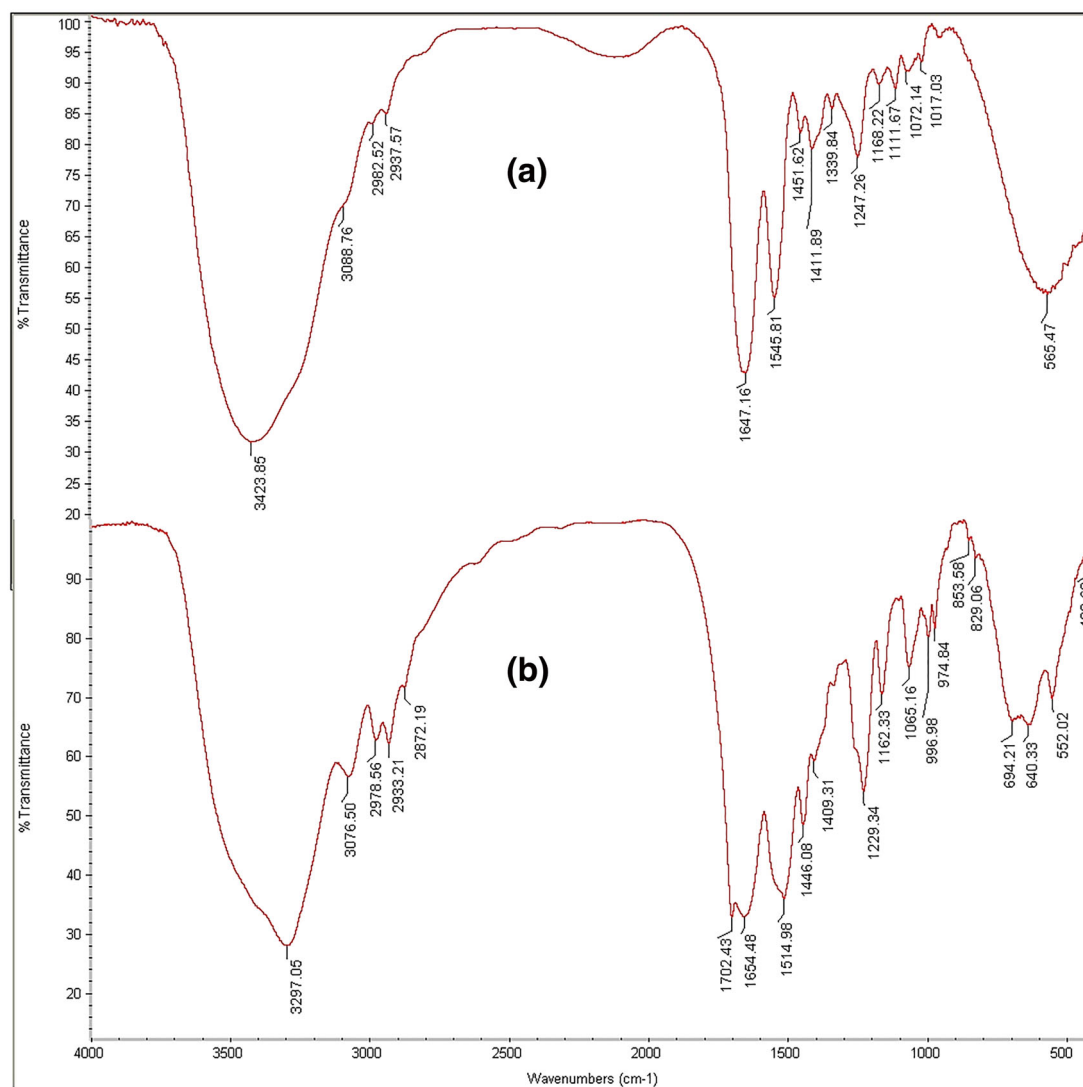


**FIGURE 1** Fourier transform-infrared (FT-IR) spectra of fibroin fibers: (a) without palladium; and (b) with palladium

comparison, spectroscopic data ( $^1\text{H-NMR}$  and MS) were also studied and showed excellent accordance.

## 2.5 | Representative spectral data for the selected products

Product **3d**: (*E*)-3-(2-methoxy-phenyl)-acrylic acid methyl ester: mass:  $m/z = 192$  ( $\text{M}^+$ );  $^1\text{H-NMR}$  (300 MHz,  $\text{CDCl}_3$ ):  $\delta$  3.83 (s, 3H,  $\text{OCH}_3$ ), 3.90 (s, 3H,  $\text{OCH}_3$ ), 6.57 (d,  $J = 15.9$  Hz, 1H, vinyl), 6.93 (d,  $J = 8.7$  Hz, 1H, Ar), 6.98 (d,  $J = 8.7$  Hz, 1H, Ar), 7.34–7.40 (m, 1H, Ar) 7.53 (dd,  $J = 7.8$  Hz, 1.5, 1H, Ar), 8.03 (d,  $J = 15.9$  Hz, 1H, vinyl).

Product **3e**: (*E*)-3-(4-methoxy-phenyl)-acrylonitrile: mass:  $m/z = 159$  ( $\text{M}^+$ );  $^1\text{H-NMR}$  (300 MHz,  $\text{CDCl}_3$ ):  $\delta$  3.87 (s, 3H,  $\text{OCH}_3$ ), 5.74 (d,  $J = 16.5$  Hz, 1H, vinyl), 6.94 (d,  $J = 8.7$  Hz, 2H, Ar), 7.36 (d,  $J = 18$  Hz, 1H, vinyl), 7.42 (d,  $J = 8.7$  Hz, 2H, Ar).

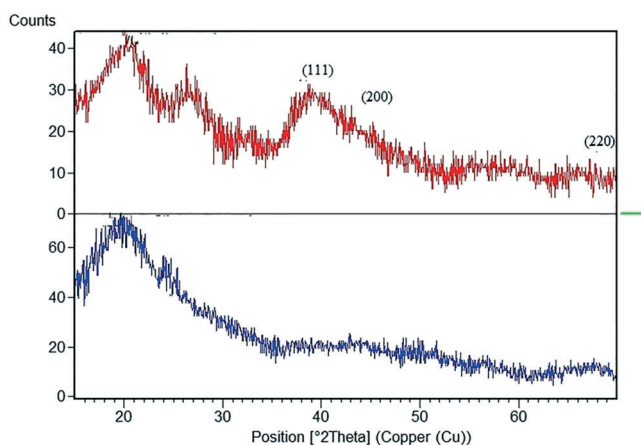


**FIGURE 2** X-ray diffraction (XRD) patterns of fibroin fibers: (a) with palladium; and (b) without palladium

Product **3i**: (*E*)-1, 2-diphenylethene: mass:  $m/z = 180$  ( $\text{M}^+$ );  $^1\text{H-NMR}$  (300 MHz,  $\text{CDCl}_3$ ):  $\delta$  7.16 (s, 1H, vinyl), 7.28–7.30 (m, 1H, Ar), 7.40 (m, 2H, Ar), 7.56 (m, 2H, Ar).

Product **3k**: (*E*)-3-(4-methoxy-phenyl)-2-methyl-acrylic acid methyl ester: mass:  $m/z = 206$  ( $\text{M}^+$ );  $^1\text{H-NMR}$  (300 MHz,  $\text{CDCl}_3$ ):  $\delta$  2.17 (d,  $J = 1.2$  Hz, 3H,  $\text{CH}_3$ ), 3.84 (s, 3H,  $\text{OCH}_3$ ), 3.87 (s, 3H,  $\text{OCH}_3$ ), 6.96 (d,  $J = 8.7$  Hz, 2H, Ar), 7.42 (d,  $J = 8.7$  Hz, 2H, Ar), 7.68 (s, 1H, vinyl).

## 2.6 | Recycling and reusing of the catalyst

Due to the fact that the catalyst is insoluble in hot DMF, it can be recycled by simple filtration. The separated catalyst was washed with hot ethanol, dried at room temperature and reused in the reaction.

## 3 | RESULTS AND DISCUSSION

### 3.1 | Characterization results of the Pd/Fib. catalyst

#### 3.1.1 | Fourier transform-infrared spectra

Pure SF (Figure 1a) presented absorption bands at  $1647\text{ cm}^{-1}$  and  $1545\text{ cm}^{-1}$  that corresponded to amide - I (C = O stretching) and amide - II (N-H bending) of silk II structural conformation ( $\beta$ -sheet). Another absorption band observed at  $1247\text{ cm}^{-1}$  corresponded to amide - III (C-N stretching), which is typically silk I conformation ( $\alpha$ -helix or random coil structure).<sup>[17]</sup> Peaks were observed at  $1411\text{ cm}^{-1}$  (due to symmetric stretching vibrations of carboxylate group) and  $1339\text{ cm}^{-1}$  (indicating the presence of methylic groups of alanine in the silk chain). The peak at  $3423\text{ cm}^{-1}$  is a symptom of the hydroxyl (-OH) stretching

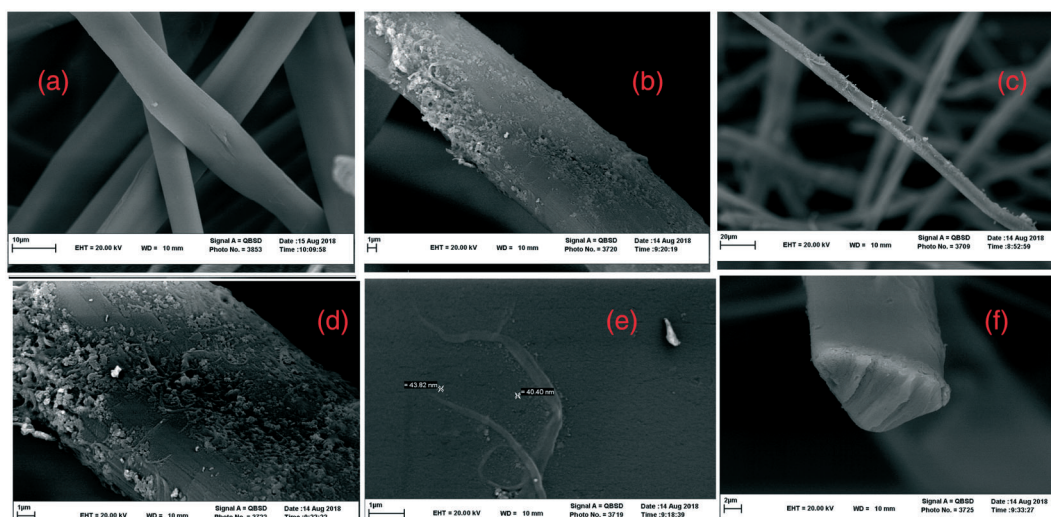


**FIGURE 3** Scanning electron microscopy (SEM) images of: (a) pure fibroin; (b) Pd/Fib.; and (c) cutting section of fibroin fiber

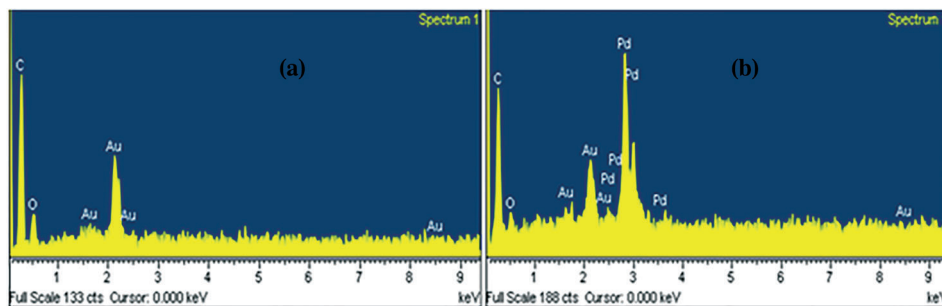


**FIGURE 4** Energy-dispersive X-ray spectroscopy (EDS) report of fibroin fibers: (a) before; and (b) after palladium loading

vibration from the phenolic acids of Tyr molecule of SF chain. Infrared (IR) analysis demonstrated that complexation of palladium by the fibroin fiber had occurred, with the prominent C-N stretching vibration of the imine ( $1247\text{ cm}^{-1}$ ) being shifted to a lower frequency ( $1229\text{ cm}^{-1}$ ) by  $18\text{ cm}^{-1}$ , indicative of metal-fibroin interaction.<sup>[17]</sup>

### 3.1.2 | X-ray diffraction

Figure 2(a) presented an X-ray diffraction (XRD) pattern typical of amorphous substances with the absence of crystallinity peaks, characterizing a silk I secondary structure.<sup>[18]</sup> The evidence of formation of Pd<sup>0</sup> NPs (Pd<sup>0</sup>/Fib.) into the surface of fibroin was obtained from powder XRD analysis. Figure 2(a) shows broad and weak peaks of  $2\theta$  values at  $40.02^\circ$ ,  $47.92^\circ$  and  $68.1^\circ$ , which are assigned to the corresponding (1 1 1), (2 0 0), (2 2 0) indices of FCC lattice of metallic Pd (JCPDS 87-0638). It can be observed that the Pd diffraction peaks were clearly weak, indicating much more homogeneous dispersion of Pd NPs in fibrous matrix.<sup>[19]</sup>

### 3.1.3 | Scanning electron microscopy

Scanning electron microscopy (SEM) images proved the high dispersion of amorphous palladium metal particles (Figure 3b,e) on the smooth surface of the SF (Figure 3 a). The palladium particles are completely dispersed throughout the surface of the fibroin fibers, but in some places their density is slightly higher, which can be seen clearly in the SEM image as crystallized dots. This homogeneous dispersion was attributed to an interaction between the Pd (OAc)<sub>2</sub> and amino acids of the SF, increasing the resistance to the growth of the Pd cluster. The elemental analysis (EDS) was employed for determination of the chemical composition of Pd/Fib. catalyst (Figure 4), and confirmed the presence of Pd in the surface of fibroin fibers. The SEM image of cutting section

of a fibroin fiber in Figure 3(c) proves that the sericin was completely removed.<sup>[20]</sup>

**TABLE 1** CHN component of fibroin fibers, before and after palladium loading

Element (%w)	Pure fibroin	Palladium/fibroin
Nitrogen	16.43	10.15
Carbon	45.24	27.86
Hydrogen	5.59	4.23

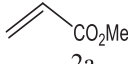
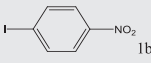
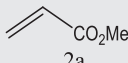
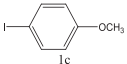
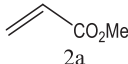
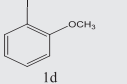
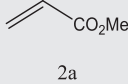
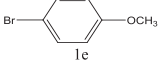
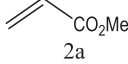
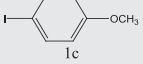
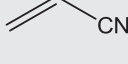
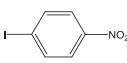
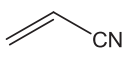
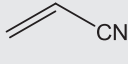
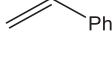
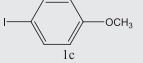
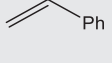
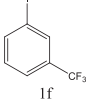
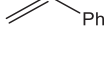
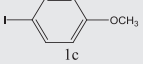
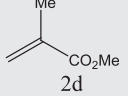
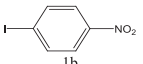
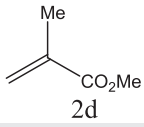
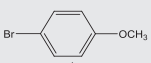
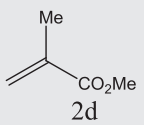
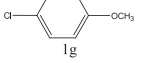
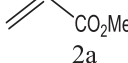
**TABLE 2** Synthesis of compound 3a in the presence of Pd/Fib. NPs as catalyst under different reaction conditions<sup>a</sup>

Entry	Catalyst (mol%Pd)			Temp. (°C)	Time (hr)	Yield (%) <sup>b</sup>
	Solvent	Base				
1	0.1	DMSO	Na <sub>2</sub> CO <sub>3</sub>	100	5	60
2	0.1	DMSO	K <sub>2</sub> CO <sub>3</sub>	100	5	65
3	0.1	DMSO	NEt <sub>3</sub>	100	5	85
4	0.1	Solvent-free	NEt <sub>3</sub>	100	4	75
5	0.1	Methanol	NEt <sub>3</sub>	reflux	5	73
6	0.1	Ethanol	NEt <sub>3</sub>	reflux	5	75
7	0.1	DMF	NEt <sub>3</sub>	100	3	90
8	0.1	DMF	NEt <sub>3</sub>	80	3	92
9	0.1	DMF	NEt <sub>3</sub>	r.t.	3	58
10	0.08	DMF	NEt <sub>3</sub>	80	3	92
11	0.05	DMF	NEt <sub>3</sub>	80	3	92
12	0.02	DMF	NEt <sub>3</sub>	80	3	86
13	–	DMF	NEt <sub>3</sub>	80	5	–

<sup>a</sup>Other conditions: iodobenzene (1 mmol), methylacrylate (1.2 mmol), triethylamine (Et<sub>3</sub>N) (1.2 mmol) as base, and DMF as solvent at 80°C.

<sup>b</sup>Isolated yield of the pure product based on iodobenzene.

**TABLE 3** Synthesis of Heck adducts **3a–3l** using Pd/Fib. NPs as catalyst under the optimized conditions<sup>a</sup>

Entry	Aryl halide	Alkene	Product <sup>b</sup>	Time (hr)	Yield (%) <sup>c</sup>
1.	 1a	 2a	3a	3	1st use:92 2nd use; 90 3rd use:87
2.	 1b	 2a	3b	3.5	89
3.	 1c	 2a	3c	3	94
4.	 1d	 2a	3d	3	92
5.	 1e	 2a	3c	5	51
6.	 1c	 2b	3e	3	92
7.	 1b	 2b	3f	3.3	89
8.	 1a	 2b	3g	3	90
9.	 1a	 2c	3h	5	85
10.	 1c	 2c	3i	5	87
11.	 1f	 2c	3j	5	83
12.	 1c	 2d	3k	3	90
13.	 1b	 2d	3l	3	88
14.	 1e	 2d	3k	6	45
15.	 1g	 2a	3c	5	33

<sup>a</sup>Reaction conditions: iodobenzene (1 mmol), methyl acrylate (1.2 mmol), triethylamine (Et<sub>3</sub>N; 1.2 mmol) as base, 0.05 mol% Pd/Fib. and DMF as solvent at 80°C.

<sup>b</sup>All the products were characterized by <sup>1</sup>H-NMR and MS.

<sup>c</sup>Isolated yield.

### 3.1.4 | Inductively coupled plasma-atomic emission spectrometry

The palladium content of Pd/Fib. catalyst was determined using the inductively coupled plasma-atomic emission spectrometry (ICP-AES) technique. This resulted in a value of about 15% w/w, and the palladium content after the third reuse in reaction was about 12% w/w.

### 3.1.5 | CHN analysis

Due to confirmation of the palladium content resulting from the ICP-AES method, the CHN content was investigated before and after palladium loading. The results are shown in Table 1, which shows that the CHN content (%w) decreased from 67.26%w to 42.24%w after palladium loading, which is approximately in accordance with the palladium content resulting from the ICP-AES method.

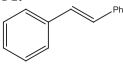
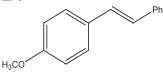
## 3.2 | Catalytic activity of the Pd/Fib. nanocatalyst in the synthesis of Heck adducts

The conditions for the Heck reaction were optimized by using iodobenzene and methylacrylate as model substrates to evaluate the effects of different solvents, type of bases, amount of catalyst and required optimum temperature of the reaction, and the results are summarized in Table 2. In the initial selection, we used dimethyl sulfoxide (DMSO) as solvent and  $K_2CO_3$  as base for the reaction in the presence of Pd<sup>0</sup>/Fib. at 100°C, whereas trans-methylcinnamate was obtained in 65% isolated yield after 5 hr. Other solvents, like methanol, ethanol and DMF, solvent-free conditions and other bases, such

as  $Na_2CO_3$  and  $Et_3N$ , were also evaluated, and DMF as solvent and triethylamine ( $Et_3N$ ) as base at 80°C yield the highest conversion (92%) among all the solvents and bases tested (Table 2, entry 11). To confirm that the activity of the Pd/Fib. catalyst is not due to leaching of the Pd NPs in solution, a model Heck reaction was conducted under optimized conditions in two reaction flasks A and B. After 1 hr of reaction, the catalyst was filtered off from both flasks A and B. At this point, isolation of the compound **3a** from flask A with column chromatography showed 40% yield of product. Further stirring of the filtrate of flask B (devoid of Pd/Fib. catalyst) for 10 hr led to no extra yield of compound **3e**, which confirms that no Pd leaching occurs in solution.

In order to evaluate the generality of this model reaction, we extended the reaction to the use of other aryl halides with other alkenes under the optimized reaction conditions. As shown in Table 3, different aryl halides (-I, -Br, -Cl) and alkenes were reacted successfully, and provided the expected products **3a–3l** in moderate to high yields with >99% trans-selectivity. However, the aryl chloride was found to be less reactive, giving the corresponding product **3c** in 33% yield (Table 3, entry 15). The iodobenzenes having electron-donating functional groups (entries 3 and 4) gave slightly higher isolated yield than electron-withdrawing groups (entry 2). Therefore, our catalyst would be efficient enough to activate the iodobenzene having electron-withdrawing groups to provide the desired products with excellent yield and selectivity. The less reactive styrene (entries 9–11) also proceeded smoothly to furnish the desired products with high yield and selectivity (i.e. >99% trans-isomer). In the case of iodobenzene with electron-withdrawing groups (entries 2, 7) and for coupling with styrene (entries 11), the reactions needed a comparatively

**TABLE 4** Comparison with previously reported catalytic systems for Heck coupling of iodobenzene or 4-iodoanisole with styrene

Entry	System, condition	Product	Yield (%)	Ref.
1	Pd/Fib., $Et_3N$ , DMF, 80°C, 3 hr, 0.05 mol% Pd	A: 	85	This work
		B: 	87	
2	CelMcPd0-1, $Bu_3N$ , DMF, 130°C, 0.8 mol% Pd	A	81	[10d]
		B	88	
3	MCNTs@(A-V)-silica-Pd, $K_2CO_3$ , TBAB, DMF, 130°C, 1.5 mol% Pd	A	91	[2b]
		B	86	
4	CB[6]-Pd NPs, $Na_2CO_3$ , DMF, 140°C, 0.5 mol% Pd, 24 hr	A	85	[21]
		B	85	
5	Pd <sup>0</sup> -Mont., $Et_3N$ , $CH_3CN$ , 82°C, 0.07 mol% Pd	A	87	[22]
		B	90	

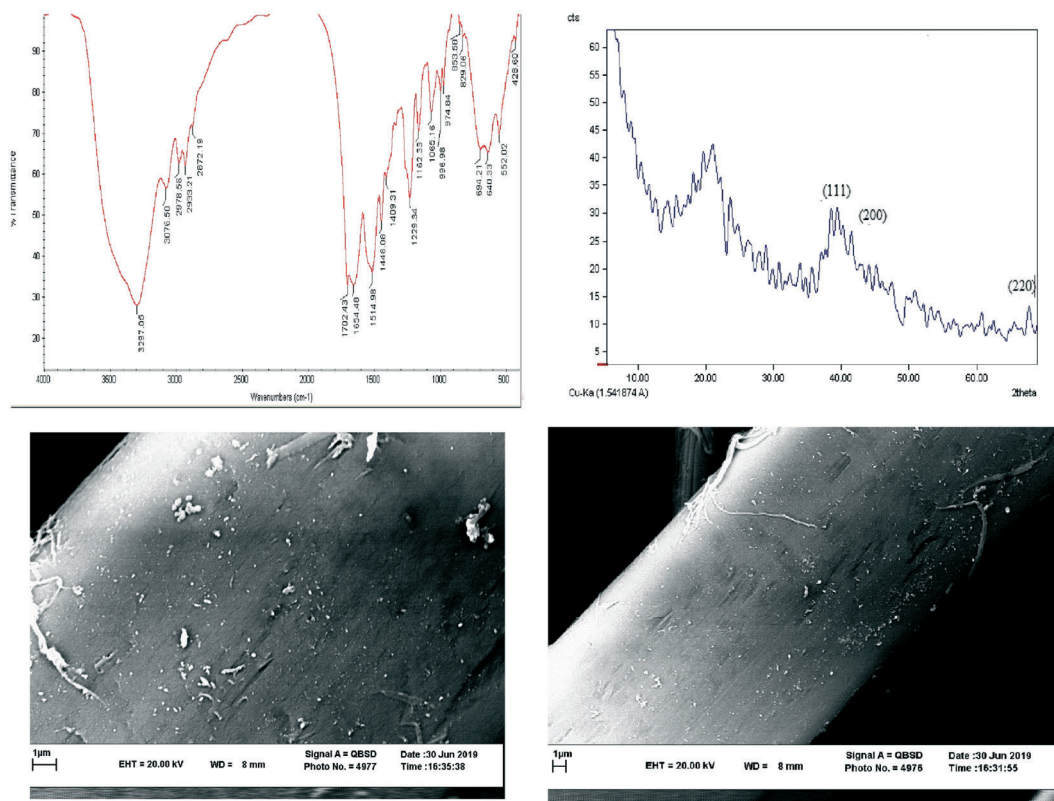


**FIGURE 5** Characterization of Pd/Fib. catalyst after recycling: (a) Fourier transform-infrared (FT-IR) spectrum; (b) X-ray diffraction (XRD) pattern; (c) and (d) scanning electron microscopy (SEM) images

longer time, i.e. 5 hr, for completion. To show the merit of the present work, the catalytic performance of the Pd/Fib. catalyst was compared with other reported catalysts<sup>[2b,10d,21,22]</sup> used in the synthesis of Heck adducts **3c** and **3i** from starting iodobenzene or 4-iodoanisole with styrene (Table 4). These comparative results establish the advantage of the Pd/Fib. catalyst over the existing methods (based on catalyst loading and reaction times). It should be noted that our catalyst's synthesis conditions were easier than the other catalytic systems mentioned in Table 4.

In order to evaluate the catalyst's useful life, the reusability of the catalyst was also investigated. For this purpose, the same model reaction was again studied under the optimized conditions. The catalyst was recovered according to the procedure mentioned in the Experimental section and reused for a similar reaction. As shown in Table 3 (entry 1), the catalyst can be used at least three times without significant loss of activity. Powder-XRD, SEM-energy-dispersive X-ray spectroscopy (EDX), Fourier transform (FT)-IR and ICP-AES were carried out to characterize the catalyst after the third recovery and reuse process, which was shown to be completely compatible with the unused catalyst structure Figure 5.

## 4 | CONCLUSION

In conclusion, we have developed a simple new catalytic method for the synthesis of Heck adducts from aryl halides and alkenes in the presence of Pd/Fib. NPs as ligand-free, efficient, reusable and heterogeneous catalysts. Some attractive features of this protocol are high yields, simple procedure, relatively short reaction times, easy work-up, high catalytic activity, and recyclability and reusability of the catalyst. The catalyst can be used at least three times.

## ORCID

Hossein Eshghi  <https://orcid.org/0000-0002-8417-220X>

## REFERENCES

- [1] R. F. Heck, J. P. Nolley, *J. Org. Chem.* **1972**, *37*, 2320.
- [2] (a) L. Jin, J. Qian, N. Sun, B. Hu, X. Hu. *Chem. Commun.* **2018**, 54, 5752. (b) D. Khalili, A. Banazadeh, E. Etemadi-Davan, *Catal. Lett.* **2017**, *147*, 2674. (c) P. Veerakumar, P. Thanasekaran, K. L. Lu, S. B. Liu, S. Rajagopal, *ACS Sustainable Chem. Eng.* **2017**, *5*(8), 6357. (d) P. Li, P. P. Huang, F.-F. Wei, Y. B. Sun, C. Y. Cao, W. G. Song, *J. Mater. Chem. A* **2014**, *2*, 12 739.

- [3] (a) A. R. Azcargorta, E. B. Coxa, I. Barbolla, E. Lete, N. Sotomayor, *Eur. J. Org. Chem.* **2016**, 2054. (b) W. Lin, K. Shia, J. Song, M. Wu, W. Li, *Org. Biomol. Chem.* **2015**, *14*, 220. <https://doi.org/10.1039/C5OB01863C> (c) M. He, Q. Ch, O. Gao, X. Hu, X. Hong, *RSC Adv.* **2015**, *5*, 16 562. (d) A. F. P. Biajoli, C. S. Schwalm, J. Limberger, T. S. Claudino, A. L. Monteiro, *J. Braz. Chem. Soc.* **2014**, *25*, 2186.
- [4] (a) F. Christoffel, T. R. Ward, *Catal. Lett.* **2018**, *148*, 489. (b) X. Chen, X. Y. Zhou, L. G. Wang, *Synthetic Comm.* **2017**, *47*, 2096. (c) M. Amini, M. Bagherzadeh, Z. Moradi-Shoeili, D. M. Boghaei, *RSC Adv.* **2012**, *2*, 12 091.
- [5] *Int. Scholarly Scientific Res Innov.* **2014**, *8*(12), 3923.
- [6] (a) B. J. Borah, D. Dutta, P. P. Saikia, N. C. Barua, D. K. Dutta, *Green Chem.* **2011**, *13*, 3453. (b) P. P. Sarmah, D. K. Dutta, *Green Chem.* **2012**, *14*, 1086. (c) I. Khan, K. Saeed, I. Khan, *Arab. J. Chem.* **2017**. <https://doi.org/10.1016/j.arabj.2017.05.011> (d) A. Alshammari, V. N. Kalevaru, A. Martin, *Green Nanotechnology – Overview and Further Prospects*. DOI: <https://doi.org/10.5772/63314>; (e) B. R. Cuenya, *Thin Solid Films* **2010**, *518*, 3127.
- [7] (a) G. Xu, L. Wang, M. Li, M. Tao, W. Zhang, *Green Chem.* **2017**, *19*, 5818. (b) Z. Wang, M. Xu, L. Shao, C. Qi, *Kinet. Catal.* **2016**, *57*, 354. (c) A. Ghorbani-Choghamarani, Z. Taherinia, *Chin. J. Catal.* **2017**, *38*, 469. (d) D. Shen, L. Chen, J. Yang, R. Zhang, Y. Wei, X. Li, W. Li, Z. Sun, H. Zhu, A. M. Abdullah, A. Al-Enizi, A. A. Elzatahry, F. Zhang, D. Zhao, *ACS Appl. Mater. Interfaces* **2015**, *7*(31), 17 450. (e) F.-X. Felpin, *Synlett* **2014**, *25*, 1055. (f) U. Akhmetzyanova, M. Opanasenko, J. Horáček, E. Montanari, J. Čejka, O. Kikhtyanin, *Microporous Mesoporous Mater.* **2017**, *252*, 116.
- [8] (a) L. Rodriguez-Perez, C. Pradel, P. Serp, M. Gomez, E. Teuma, *ChemCatChem* **2011**, *3*, 749. (b) A. Kilic, E. Gezer, F. Durap, M. Aydemir, A. Baysal, *J. Organometal. Chem.* **2019**, *896*, 129. (c) K. Köhler, M. Wagner, L. Djakovitch, *Catal. Today* **2001**, *66*, 105.
- [9] (a) M. Singh, C. Musy, E. S. Dey, C. Dicko, *Fibers Polym.* **2017**, *18*, 1660. (b) A. Shaabani, Z. Hezarkhani, E. Badali, *Polyhedron* **2016**, *107*, 176. (c) C. S. Shivanandaa, B. Lakshmeesha Raoa, A. Pashab, Y. Sangappa, *Mater. Sci. Eng.* **2016**, *149*, 012175.
- [10] (a) P. Kaur, B. Kumar, V. Kumar, R. Kumar, *Tetrahedron Lett.* **2018**, *59*, 1986. (b) T. Baran, *J. Colloid Interface Sci.* **2017**, *496*, 446. (c) S. Chairam, W. Konkamdee, R. Parakhun, *J. Saudi Chem. Soc.* **2017**, *21*, 656. (d) F. Chen, M. Huang, Y. Li, *Ind. Eng. Chem. Res.* **2014**, *53*, 8339.
- [11] (a) D. Magri, G. Caputo, G. Perotto, A. Scarpellini, E. Colusso, F. Drago, A. Martucci, A. Athanassiou, D. Fragouli, *ACS Appl. Mater. Interfaces* **2018**, *10*, 651. (b) A. N. Mitropoulos, F. J. Burpo, C. K. Nguyen, E. A. Nagelli, M. Y. Ryu, J. Wang, R. K. Sims, K. Woronowicz, J. K. Wickiser, *Materials* **2019**, *12*, 894. (c) Y. Xia, J. Wan, Q. Gu, *Gold Bull.* **2011**, *44*, 171. (d) H. Su, J. Han, Q. Dong, D. Zhang, Q. Guo, *Nanotechnology* **2008**, *19*, 025601. (e) J. Xu, H. Su, J. Han, Y. Chen, W. Song, Y. Gu, W.-J. Moon, D. Zhang, *Appl. Phys. A Mater. Sci. Process.* **2012**, *108*, 235. (f) K. Bhuvaneswari, R. D. Bharathi, T. Pazhanivel, *Mater. Res. Express* **2018**, *5*, 024004. (g) P. Ajitha, K. Vijayalakshmi, M. Saranya, T. Gomathi, K. Rani, P. N. Sudha, S. Anil, *Int. J. Biol. Macromol.* **2017**, *104*, 1469.
- [12] (a) Y. Qi, H. Wang, K. Wei, Y. Yang, R. Y. Zheng, I. S. Kim, K. Q. Zhang, *Int. J. Mol. Sci.* **2017**, *18*, 237. (b) M. Mondal, K. Trivedy, S. Nirmal Kumar, *Caspian J. Env. Sci.* **2007**, *5*, 63.
- [13] L. Koh, Y. Cheng, C. Teng, Y. Khin, X. Loh, S. Tee, M. Low, E. Ye, H. Yu, Y. Zhang, M.-Y. Han, *Prog. Polym. Sci.* **2015**, *46*, 86.
- [14] (a) B. B. Peksen, C. Uzelakcil, A. Gunes, O. Malay, O. Bayraktar, *J. Chem. Technol. Biotechnol.* **2006**, *81*, 1218. (b) B. Liu, Y. Song, L. Jin, Z. Wang, D. Pu, S. Lin, C. Zhou, H. You, Y. Ma, J. Li, L. Yang, K. L. Sung, Y. G. Zhang, *Colloid Surf. B Biointerfaces* **2015**, *131*, 122.
- [15] (a) Q. Liu, X. Wang, X. Tan, X. Xie, H. Dong, X. Li, Y. Li, P. Zhao, Q. Xia, *Int. J. Mol. Sci.* **2019**, *20*(12), 3026. (b) K. Bhuvaneswari, R. Divya Bharathi, T. Pazhanivel, *Mater. Res. Express* **2018**, *5*, 024004.
- [16] (a) H. Sajiki, T. Ikawa, H. Yamada, K. Tsubouchib, K. Hirotaa, *Tetrahed. Lett.* **2003**, *44*, 171. (b) S. Das, B. B. Dhar, *RSC Adv.* **2014**, *4*, 46 285. (c) Y. Lei, Q. Shi, C. Han, B. Wang, N. Wu, H. Wang, Y. Wang, *Nano Res.* **2016**, *9*, 2498.
- [17] (a) S. Lu, J. Li, S. Zhang, Z. Yin, T. Xinga, D. L. Kaplanb, *J. Mater. Chem. B* **2015**, *3*, 2599. (b) H. Zhang, L. L. Li, F. Y. Dai, H. H. Zhang, B. Ni, W. Zhou, X. Yang, Y. Z. Wu, *J. Transl. Med.* **2012**, *10*, 117.
- [18] (a) K. Sen, M. Babu, *K. J. App. Poly. Sci.* **2004**, *92*, 1098.
- [19] H. Veisi, S. A. Mirshokraee, H. Ahmadian, *Int. J. Biol. Macromol.* **2018**, *108*, 419.
- [20] (a) B. J. Allardyce, R. Rajkhowa, R. J. Dilley, M. D. Atlas, J. Kaur, X. Wang, *Text. Res. J.* **2015**, *86*, 275. (b) J. Wang, W. Wong, *J. Stud. Conservation* **2019**, *64*, 125.
- [21] M. Cao, Y. Wei, S. Gao, R. Cao, *Catal. Sci. Technol.* **2012**, *2*, 156.
- [22] B. J. Borah, D. K. Dutta, *J. Mol. Catal. A Chem.* **2013**, *366*, 202.

**How to cite this article:** Mirzaei H, Eshghi H, Seyedi SM. Finely dispersed palladium on silk-fibroin as an efficient and ligand-free catalyst for Heck cross-coupling reaction. *Appl Organometal Chem.* 2019;e5231. <https://doi.org/10.1002/aoc.5231>